International Conference on Applied Energy 2019
Aug 12-15, 2019, Västerås, Sweden
Paper ID: 0099

EXPERIMENTAL INVESTIGATION OF ORGANIC RANKINE CYCLE (ORC) SYSTEM WITH DIFFERENT COMPONENTS

L. Li[1], Y.T. Ge [2*], X. Luo[3] and S. A. Tassou[4]

1 School of Engineering and Computer Sciences, University of Hertfordshire, Hatfield, Hertfordshire, AL10 9AB, UK

2 Sustainable Environment Research Centre, Faculty of Computing, Engineering and Science, University of South Wales, Pontypridd, CF37 1DL (Corresponding Author)

3 National Key Laboratory of Science and Technology on Aero Engines Aero-thermodynamics, The Collaborative Innovation Centre for Advanced Aero-Engine of China, Beihang University, Beijing, 10191, China

4 RCUK National Centre for Sustainable Energy Use in Food Chains (CSEF), Institute of Energy Future, Brunel University London, Uxbridge, Middlesex, UB8 3PH, UK

ABSTRACT

In this study, a small-scale test rig of organic Rankine cycle (ORC) system driven by low-grade heat has been developed and investigated experimentally. The test rig consisted of a number of essential components including a scroll expander and squirrel cage motor, plate-type recuperator, finned-tube air cooled condenser, liquid receiver, liquid pump, two thermal oil heated evaporators and other ancillaries. Considering its zero ozone depletion potential and appropriate thermophysical properties, R245fa was selected as a working fluid in the ORC system. Correspondingly, R245fa flow was heated and evaporated through either a plate-type evaporator or a shell and tube one by hot thermal oil flow which itself was circulated and heated by exhausted flue gases from an 80 kW_e microturbine CHP unit. In this paper, the experimental investigations were mainly carried out on the ORC system with different evaporators and with or without recuperator integrated. Subsequently, the effects of various types of evaporators and with or without recuperator on the system performance are evaluated, compared and analysed. The test results and analysis are essential to understand the system operation at different design structures and components which can significantly contribute towards optimal component selections and system performance controls.

Keywords: R245fa Organic Rankine Cycle; Experiment; Scroll expander; Evaporator

1. INTRODUCTION

Globally, the extensive consumption of fossil fuels in power generation has been contributing increasingly to global warming, air pollution and energy resource depletion. One of the global challenges is to tackle these risks surrounding excessive CO_2 emissions in power generation by replacing fossil fuels with low grade waste heat recovery systems and applicable thermodynamic power cycles such as Organic Rankine Cycles (ORCs) [1]. However, the performance of an ORC system still needs to be further improved.

The working mechanism of an ORC is very similar to a conventional steam Rankine cycle for power generation, but instead an organic fluid such as R245fa is used as the working fluid, which is able to evaporate at higher temperature and condense at lower temperature. The working fluid was selected due to its zero ozone depletion potential (ODP), however, it has been taken into consideration that the fluid has high global warming potential (GWP). When applied into a low grade heat source, the system with ORC is expected to generate power with higher efficiency and more cost effective than that of steam Rankine cycle [2]. However, the most challenge tasks on an ORC system are how to select an appropriate working fluid and its associated components. Saleh et al. [3] compared theoretically the system performance of ORCs with thirty-one pure working fluids. The thermal efficiencies of the ORCs were calculated with range between 0.36% and 13%, while

R245fa ORC could present approximately 12.52% efficiency. Li et al. [4] conducted a simulation study on performance comparisons of R245fa organic Rankine cycles and CO_2 transcritical power cycles with different heat source temperatures, heat sink temperatures and evaporating pressures. The results showed that the thermal efficiencies of both cycles can be enhanced by installing a recuperator in each system at specified operating conditions. An experimental investigation was carried out by Wang et al. [5] on a low-temperature solar recuperative Rankine cycle system using working fluid R245fa and a flat plate collector was used as evaporator for gathering solar energy. The test results demonstrated that the introduction of recuperator in the ORC system could not increase the system thermal efficiency. This was because that the preheating by the expander exhaust through the recuperator lowered the solar collector efficiency and thus the overall system thermal efficiency. The ORC system thermal efficiencies for the above cases were calculated using the same methodology which comprised of cycle performance. Another disadvantage of recuperator integration in an ORC system is the pressure increase at the expander outlet due to fluid pressure drop through the heat exchanger, which will affect negatively the expander efficiency. The pressure drop through the recuperator however is subject to the working fluid flow rate and therefore different components and system operating states which need to be further investigated experimentally.

In this investigation, a small-scale test rig of R245fa ORC system using hot thermal oil as a heat source was constructed and instrumented. The test rig consists of a scroll expander with generator, plate-type recuperator, finned-tube air cooled condenser, liquid receiver, liquid pump, plate-type evaporator and shell and tube evaporator. The effects of ORC system with different evaporators and with or without recuperator on the performances of scroll expander and system were examined experimentally. The experimental investigation can provide a significant guidance to understand the performances of ORC system with different components and therefore optimize the ORC system designs and operations.

2. EXPERIMENTAL SYSTEM AND FACILITIES

A schematic diagram of the small-scale R245fa ORC test rig is presented in Fig. 1. The system consisted of two operational loops: ORC and heat source. The ORC loop comprised of two oil heated evaporators connected in parallel (shell and tube evaporator and plate-type evaporator), an R245fa scroll expander with squirrel cage generator, plate-type recuperator, finned-tube air cooled condenser, liquid receiver, liquid pump and other ancillary equipment. For the shell and tube evaporator, the ORC fluid was on the shell side while the thermal oil was on the tube side. As to the plate evaporator, the ORC fluid was on the left side flowing from bottom to top while the thermal oil was on the right side passing from top to bottom. On the other hand, two restrictive valves were installed at each side of the recuperator so that the ORC could either flow through or bypass the recuperator. Subsequently, the system performance with different evaporators and with and without recuperator could be evaluated and compared experimentally. After one of the evaporators, the superheated vapor flowed through the scroll expander and thus drove a generator to generate electricity power. As illustrated in Fig. 2(a), the generator was connected to break resistors so as to investigate the expander performance at variable electric loads. The scroll expander was a positive displacement with lubricant oil free and established by two identical spiral-shaped scrolls fixed on a back plate. The stationary scroll had ports in the back plate while the orbiting scroll moved in a circular path. The superheated working fluid entered the central chamber through the fixed back plate center inlet port and exited from the chamber exhaust through the outlet port of the back plate. Therefore, the scroll expander can be classified as kinematically constrained.

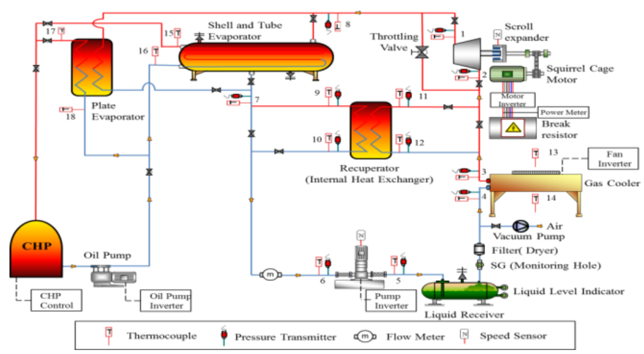

Fig 1 Schematic representation of the ORC test rig.

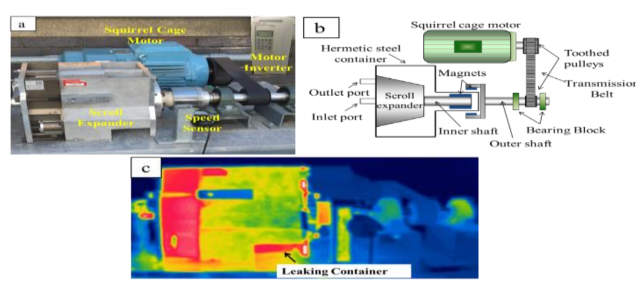

Fig 2 Photographs of the scroll expander with squirrel cage motor and details.

As shown in Fig. 2(b), the scrolls were installed inside a rigid steel container and the inner shaft didn't go through the orbiting scroll plate. The power was then transferred from the inner shaft to an outer shaft by means of a magnetic coupling. At such a circumstance, the scroll expander did not require any auxiliary power supply. As shown in Fig. 2 (c), the working fluid leaked from both internal and external was collected inside of the steel container which flowed together with the main working fluid stream. Connected to the outer shaft, an asynchronous machine was driven by the scroll expander through a belt-and-pulley coupling. Using the asynchronous machine was a suitable way to impose the rotational speed of the scroll expander, which could be adjusted by means of an ABB 4-quadrant inverter. Therefore the asynchronous machine could be able to run both motor and electric generator modes. From the scroll expander outlet, the R245fa low pressure vapor flew directly into a 17 kW plate-type recuperator or a finned-tube air cooled condenser. The ambient air was used as a heat sink for the test rig. Therefore, the air mass flow through the finned-tube air cooled condenser was adjusted by a speed controlled fan so that the required condensation temperature and pressure can be achieved. Furthermore, the ORC working fluid mass flow rate and evaporating pressure of the test rig could be controlled by the adjusting the rotation speed of a seal-less diaphragm type pump.

For the heat source loop, the thermal oil flow was firstly heated by exhaust gases of an 80 kW_e CHP unit and then pumped to one of the evaporators installed in parallel to heat and evaporate the ORC fluid. The thermal oil was then circulated back and heated by the CHP exhaust gases again. The CHP unit had been already installed at Brunel University London. An exhaust gas-thermal oil boiler was installed in the CHP unit to recover waste heat from the exhaust gases and transfer to the thermal oil loop, which is the main heat source for the ORC loop. The thermal oil temperature was adjusted by means of the CHP power output controls [6] while the thermal oil flow rate was modulated by a variable frequency drive attached to the oil pump (cf. Fig.1). In addition, the test rig was fully instrumented with calibrated sensors, flow and power meters, as shown in Fig. 1. The parameters, types, ranges and accuracies of these instruments are also listed in Table 1.

Parameter	Type	Range	Accuracy
Temperatures	Type-K thermocouple	(-10)~1100 ºC	±0.5 ºC
Pressures	RPS	0~25 bar	±0.3%
Flowmeter	Twin tube type	0~6500 kg/h	±0.15%
Pump and Expander Rotation Speed	Laser Speed Sensor	50~6000 RPM	±0.75%
Electric Power Meter	Digital multimeter	1mW~8kW	±0.8%
Ambient Air Velocity	Hot Wire Anemometer	1.27~78.7 m/s	±0.15m/s

Table 1 Measuring range of precision of the applied sensors.

3. EXPERIMENTAL RESULTS AND DISCUSSIONS

Once the test rig was setup, experimental investigation could be carried out to evaluate and compare the system performance at different structural layouts and operating conditions. Parameters of temperatures, pressures and fluid mass flow rates for both sides of the ORC working fluid (R245fa) and heat source (thermal oil) were measured and recorded by a data logger system at each steady state. In addition, the power generation from the scroll expander and power input from the R245fa liquid pump were also measured. The scroll expander power outputs were measured directly using a power meter installed at outlet electric wire of the power generator in both conditions. All the thermophysical properties of R245fa such as enthalpy and entropy etc. were calculated using REFPROP 8.0 software [7] based on the average measured temperature and pressure at each measured point. In order to examine the performance of the scroll expander at different pressure ratios, a series of tests were carried out for the system with either shell and tube evaporator or plate evaporator, with or without the recuperator. As listed in Table 2, the measured parameters for the

Evaporator type	Recuperator	Range	$P_{ex,in}$ (bar)	$P_{ex,out}$ (bar)	Pressure ratio	$T_{ex,in}$ (ºC)	$\dot{M}$ (kg/s)	$T_{ex,out}$ (ºC)	$\dot{W}_{el}$ (W)	$\dot{W}_p$(W)
Shell and tube	with	Min	10.01	4.34	2.31	93.93	0.1278	68.99	689.93	67.69
		Max	11.6	4.49	2.58	120	0.1416	96.23	1195.12	95.32
	without	Min	8.73	4.03	2.17	87.07	0.1328	57.02	395.05	62.67
		Max	9.64	4.06	2.37	93.42	0.1354	69.57	802.43	73.85
Plate-type	with	Min	7.02	3.12	2.25	77.22	0.1224	48.74	288.16	52.24
		Max	10.58	3.25	3.26	157.38	0.1275	124.94	1556.42	92.96
	without	Min	9.48	3.11	3.05	109.95	0.1207	81.85	1174.79	78.36
		Max	10.45	3.25	3.22	156.71	0.1251	122.85	1443.78	87.36

Table 2 Ranges of the main measured variables for scroll expander.

expander include the variations of temperatures and pressures at the expander inlet and outlet, ORC fluid mass flow rates, expander power generations and pump power consumptions. The pressure ratio is also calculated and listed in the table. It is seen from that table that the ORC fluid flow rates and expander outlet pressures were all mostly higher for the test system with shell and tube evaporator than those with plate evaporator but the pressure ratios are relatively lower. Consequently, the power generations for the system with plate evaporator were relatively higher than those of system with shell and tube evaporator. Although it is not clear which evaporator matched well in the system, the system test results with different component combinations can provide extensive data to evaluate the expander and system performances.

From the test results, the variations of expander power generation and pump power consumption with expander pressure ratios are depicted in Fig. 3. It is seen that the expander power generation increases polynomially with higher expander pressure ratio which could be correlated as indicated in the diagram. On the other hand, the pump power consumption increases linearly with higher expander pressure ratio. Additionally, the system with plate evaporator presents the test results with the whole range of pressure ratios while only smaller pressure ratios are covered by the test results of system with shell and tube evaporator. When the pressure ratios are within the lower range, at a constant pressure ratio, the expander power generation and pump power consumption are both relatively higher for the system with shell and tube evaporator.

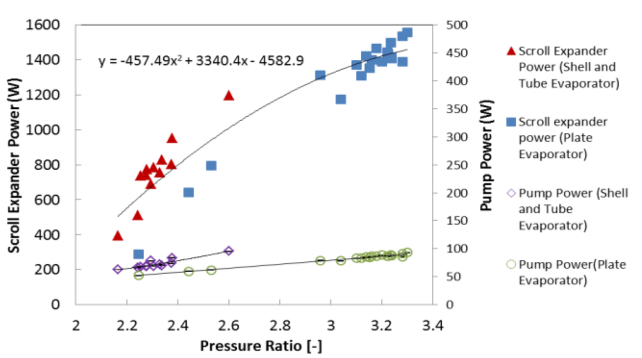

Fig 3 Variations of scroll expander and pump powers with expander pressure ratio for the system with various evaporators and with and without recuperator

To clarify, the expander overall efficiency ($\eta_{exp.all}$) and system overall efficiency ($\eta_{s,all}$) are defined and calculated as:

$$\eta_{exp,all} = \frac{W_{exp}}{m_f(h_1-h_{2,is})};\ \eta_{s,all} = \frac{W_{exp}-W_p}{m_f(h_8-h_7)}$$

In the above equations, W_{exp} (kW); W_p (kW), $\dot{m}_f$ (kg/s) are the measured power generation, R245fa pump power consumption, R245fa mass flow rate; the *h* is enthalpy (kJ/kg) and the subscript numbers correspond to the diagram in Fig 1 while "*is*" means isentropic expansion process.

Subsequently, the variations of expander overall efficiency with pressure ratio are calculated and plotted in Figure 4 (a). In this figure, the calculation for expander overall efficiency indicates the results of system with and without recuperator. Similar to that of expander power generation, when the pressure ratio is less than 3, the overall efficiency increases polynomially with higher pressure ratio and decreases with the pressure ratio if the pressure ratio increases further. Therefore, there is a maximum expander overall efficiency when the pressure ratio is around 3. Again the relation between the overall efficiency and pressure ratio can be correlated and indicated in the same diagram. To evaluate and compare the effect of recuperator installation on the system performance, the variations of system overall efficiency with expander pressure ratios for the system with different evaporators, with or without recuperator are demonstrated in Figure 4 (b). As seen in Figure 4(b), the system overall efficiency also increases polynomially with higher expander pressure ratio regardless the system structures. However, the system with shell and tube evaporator can only operate in a lower range of pressure ratios while the system with plate evaporator is able to work in a larger range of pressure ratios. For this figure, the system with plate evaporator mainly shows a higher range of pressure ratios. Consequently, the system overall efficiency is higher when the plate evaporator is utilized. On the other hand, the system overall efficiency can be greatly improved when a recuperator is applied due to the reduction of heat input to the ORC system. It is also noted that the system overall efficiency can reach above 5% at pressure ratio 3.3 when a plate evaporator and a recuperator are employed in the system.

Figure 5 presents the results of the scroll expander power generation and the system overall efficiency at different evaporator heat capacities and with and without recuperator. It is noted that the scroll expander power generation and system overall efficiency both increase with higher evaporator heat capacity irrespective of the system compositions. However, the

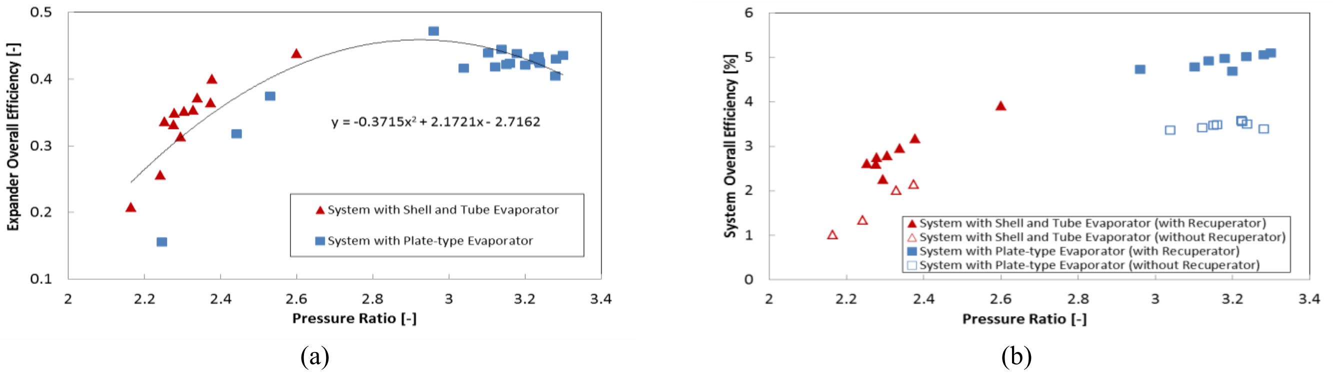

Fig 4 Variations of scroll expander overall efficiency (a) and system overall efficiency (b) with expander pressure ratio for the system with various evaporators and with and without recuperator

system with recuperator can operate at a lower required evaporator heat capacity while both expander power generation and system overall efficiency are higher when plate evaporator is employed. The measurements can also illustrate that the integration of recuperator can greatly improve the ORC system performance in terms of power generation, system overall efficiency and evaporator heat capacity required.

4. CONCLUSIONS

A small-scale R245fa ORC test rig was developed to investigate the performance characteristics of ORC systems under different conditions and system component compositions. These included a scroll expander, two types of evaporators including shell and tube and plate ones, with and without recuperator integrated. Thermal oil was used as a heat source for the ORC system which was heated by the exhaust flue gases from an 80 kWe CHP unit. The system could operate at a large range of expander pressure ratios contributed by different evaporators used in which the system with shell and tube evaporator operated at lower range of pressure ratio while the system with plate evaporator could work at larger range of pressure ratio. It is seen from the measurements that the expander power generation increases polynomially with higher pressure ratio while the expander overall efficiency increases with higher pressure ratio if it is not too high and decreases if the pressure ratio growths further. This indicates that there is an optimal pressure ratio to maximize the expander overall efficiency. In addition, the system overall efficiency also increases polynomially with higher pressure ratio and it can be greatly improved when a recuperator is employed irrespectively of the type of evaporator employed. The benefit of system performance from the recuperator integration is due to its contribution to the reduction of required evaporator heat capacity and the reduction of the required condenser capacity for the same condenser conditions. On the other hand, for a fixed system structure and component composition, both expander power generation and system overall efficiencies increase with higher evaporator heat capacity. But if the heat capacity is not quite high, the power generation and system overall efficiency are both higher when a plate evaporator and recuperator are employed compared to those with a shell and tube evaporator and recuperator. The research outcomes from this paper can contribute significantly to the understanding of scroll expander

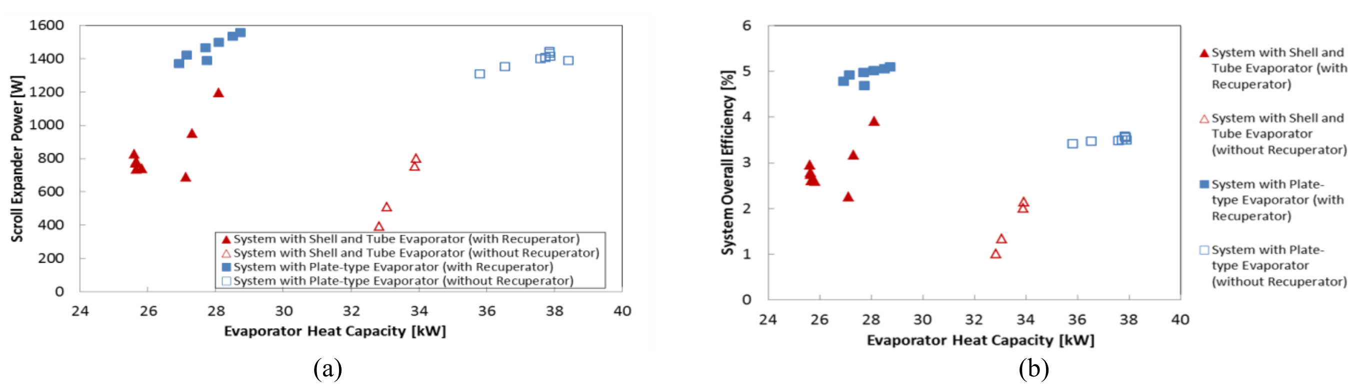

Fig 5 Variations of scroll expander power (a) and system overall efficiency (b) with different evaporator heat capacities and with and without recuperator

operation at different pressure ratios and the effects of different types of evaporators and recuperator integrations on the system performance. It can therefore direct the ORC system designs and controls.

REFERENCE

[1] Li L, Ge YT, Luo X, Tassou SA. Experimental investigations into power generation with low grade waste heat and R245fa Organic Rankine Cycles (ORCs). Applied Thermal Engineering. 2017; 115:815-824.

[2] Hajabdollahi Z, Hajabdollahi F, Tehrani M, Hajabdollahi H. Thermo-economic environmental optimization of Organic Rankine Cycle for diesel waste heat recovery. ENERGY. 2013; 63:142-151.

[3] Saleh B, Koglbauer G, Wendland M, Fischer J. Working fluids for low-temperature organic Rankine cycles. Energy. 2007; 32:1210-1221.

[4] Li L, Ge Y, Luo X, Tassou S. Thermodynamic analysis and comparison between CO2 transcritical power cycles and R245fa organic Rankine cycles for low grade heat to power energy conversion. APPLIED THERMAL ENGINEERING. 2016; 106:1290-1299.

[5] Wang JL, Wang XD, Zhao L. An experimental study on the recuperative low temperature solar Rankine cycle using R245fa. Applied Energy. 2012; 94:34-40.

[6] Ge YT, Tassou SA, Chaer I, Suguartha N. Performance evaluation of a tri-generation system with simulation and experiment. Applied Energy. 2009; 86:2317-2326.

[7] Lemmon E, Huber M, McLinden M. NIST REFPROP standard reference database 23. Version 8.0. User's guide. NIST. 2007.